Viscoelastic Behavior of Poly(ether imide) Incorporated with Multiwalled Carbon Nanotubes

Kimberly B. Shepard,[1]* Halil Gevgilili,[2] Miguel Ocampo,[1]† Jia Li,[1]‡ Frank T. Fisher,[3] Dilhan M. Kalyon[1,2]

[1]Department of Chemical Engineering and Materials Science, Stevens Institute of Technology, Castle Point on Hudson, Hoboken, New Jersey 07030

[2]Highly Filled Materials Institute, Stevens Institute of Technology, Castle Point on Hudson, Hoboken, New Jersey 07030

[3]Department of Mechanical Engineering, Stevens Institute of Technology Castle Point on Hudson, Hoboken, New Jersey 07030

Correspondence to: D. M. Kalyon (E-mail: dkalyon@stevens.edu)

Received 6 July 2012; accepted 31 July 2012; published online 8 September 2012
DOI: 10.1002/polb.23151

ABSTRACT: There is significant potential in improving the mechanical, electrical, and thermal properties of engineering plastics, including poly(ether imide) (PEI), with various nanoinclusions such as multiwalled carbon nanotubes (MWCNTs). However, this potential can only be fully realized through a thorough understanding of the rheological behavior and the thermomechanical histories that the nanocomposites are exposed to during their preparation and the resulting effective properties. In this study, nanocomposites of PEI and MWCNTs were prepared using a solution processing method under different dispersion conditions, and the viscoelastic material functions of the nanocomposites were characterized as functions of concentration of CNTs in the 1–5% by weight range (volume fraction, $\phi = 0.006$–0.03) and temperature. The storage modulus and magnitude of complex viscosity values of the PEI nanosuspensions increased by as much as 3500% and 800%, respectively, at $\phi = 0.03$, along with similar orders of magnitude increases observed or predicted in other viscoelastic material functions. Such increases reflect how nanotube incorporation and network formation can drastically alter the flow and deformation behavior of the PEI/CNT nanosuspensions at processing-relevant temperatures and deformation rates. © 2012 Wiley Periodicals, Inc. J Polym Sci Part B: Polym Phys 50: 1504–1514, 2012

KEYWORDS: polyethers; processing; relaxation; rheology; thermoplastics; viscoelastic properties

INTRODUCTION The demand for lightweight materials with high strength and thermal and chemical stability is ever increasing. Poly(ether imide) (PEI), which is considered to be an engineering plastic, and suitable for use in many demanding applications because of its relatively high strength, high glass transition temperature (216–220 °C), and low degradation rates at temperatures as high as 500 °C.[1] Furthermore, there is a significant potential in further enhancing the ultimate properties of PEI by functionalizing it with various nanoparticles.

Carbon nanofibers (CNFs) and multiwalled carbon nanotubes (MWCNTs)[2] have been widely used in recent years as polymer functionalization agents because of their exceptional mechanical, electrical, and thermal properties. Polymers that have been modified with CNTs or CNFs, and for which enhancements of mechanical and electrical properties are observed, include poly(propylene),[3–5] poly(methyl methacrylate),[6,7] poly(ethylene terepthalate),[8] poly(carbonate),[9,10] poly(ethylene),[11] poly(imide),[12] and poly(ether ether ketone) (PEEK).[13] Furthermore, an increase of the glass transition temperature is often observed with the incorporation of CNTs, for example, a 10 °C increase has been reported for poly(methyl methacrylate) incorporated with 4% CNT by weight.[7] At relatively low concentrations of CNT, the electrical percolation occurs on the basis of the formation of a volume-spanning network of the conductive nanotubes. The typical aspect ratios of nanotubes in the 100–2100 range enable electrical percolation at CNT volume fractions as low as 0.05%.[9,12] For semicrystalline matrices, the incorporation of the nanoinclusions can also alter the distributions of the different types of polymorphs in the crystalline phase of the polymer matrix,[14,15] for example, increasing the concentration of the β-polymorph in poly(vinylidene fluoride) that exhibits piezoelectric, ferroelectric, and pyroelectric properties.[15]

There are a number of earlier investigations that have probed the development of electrical,[1,16] mechanical,[1,17] and

*Present address: Kimberly B. Shepard, Department of Chemical and Biological Engineering, Princeton University, Princeton, New Jersey.
†Present address: Miguel Ocampo, The Shaw Group, Energy and Chemicals Group, Stoughton, Massachusetts.
‡Present address: Jia Li, ECI Technology, Inc., Totowa, New Jersey.

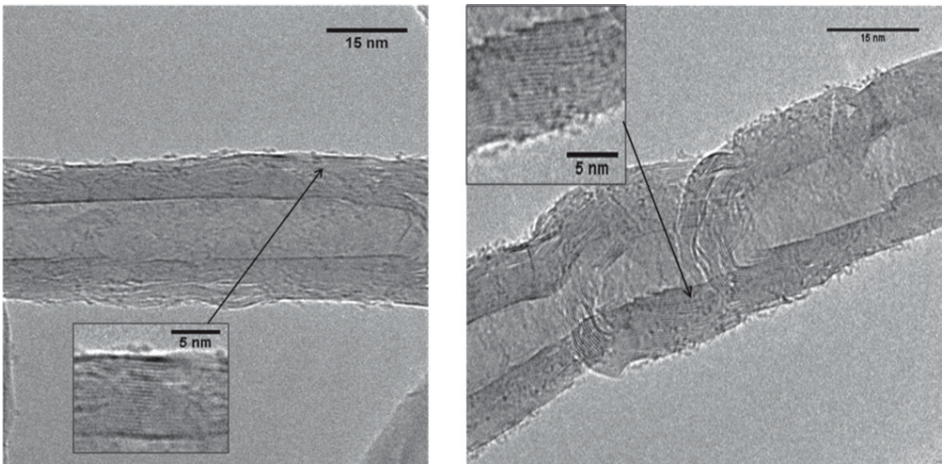

FIGURE 1 TEM micrographs of as-received multiwalled carbon nanotubes (MWCNTs) (a) and MWCNTs with surface functionalization (b).

thermal properties[1,16,17] of PEI nanocomposites. Kumar et al.[1] have prepared PEI/CNF composites using an internal mixer, followed by compression molding. Results from thermogravimetric analysis (TGA) have shown that thermal decomposition temperature decreased 4% with the addition of 3% by weight of as-received CNF. The glass transition temperature determined via dynamic mechanical analysis was observed to increase by 8 °C, that is, from 214 to 222 °C on the incorporation of 3% by weight of surface-functionalized CNFs. Additionally, the mechanical properties of PEI were not affected significantly by the incorporation of the CNF.[1] Kumar et al.[16] later reported a solvent-based process that produced a 12 order of magnitude increase in electrical conductivity and increase in glass transition temperature and 85 °C increase in decomposition temperature with 0.5% by weight of functionalized CNT.[16] Liu et al. have also studied PEI as a matrix for nanocomposites by generating ultrathin PEI/CNT films by mixing MWCNTs into poly(amic acid) under vigorous stirring, followed by casting onto glass slides and high-temperature curing to induce an imidization reaction. The glass transition temperature of the PEI/CNT nanocomposite (at 1% by weight of CNT) was observed to increase by 11 °C, that is, from 218 to 229 °C, and the storage modulus was observed to increase by ~150% at room temperature.[17]

The significant changes in mechanical and electrical properties of polymers compounded with modest concentrations of CNT rely on the adequate dispersion of the CNT in the polymer matrix.[18,19] The aspect ratio and the concentration of the CNT and their state of dispersion affect the rheological behavior of the CNT/polymer suspension. Furthermore, despite the industrial importance of PEI, there are no previous studies that have focused on the rheological behavior of PEI incorporated with differing concentrations of CNT. Such data are particularly valuable considering the narrow and relatively high-temperature processing window of PEI, that is, at temperatures >370 °C.[20] Here, we report our findings on the viscoelastic behavior of PEI and PEI/CNT suspensions in the CNT weight percent range of 1–5%. Dynamic properties were characterized over a broad range of temperatures along with relaxation modulus data in the linear viscoelastic range and elucidated in conjunction with a linear viscoelastic constitutive equation. The relaxation spectra determined from the dynamic properties were combined with a damping function, parameters of which were characterized from step-strain experiments, to predict the shear viscosity and first normal stress coefficient material functions via a nonlinear integral viscoelastic constitutive equation (K-BKZ with Wagner postulate) at the relatively high shear rate ranges that are not accessible experimentally, but are of utmost importance in industrially relevant processing conditions.

EXPERIMENTAL

Materials

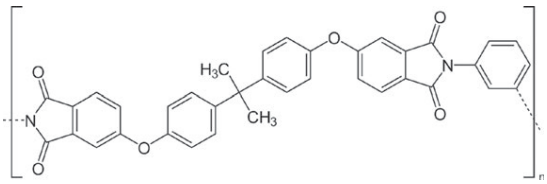

The multiple aromatic rings of PEI give rise to a stiff backbone and consequently a relatively high glass transition temperature of 216–220 °C. The PEI resin used in the investigation has a specific gravity of 1.27 and was obtained from Sabic Innovative Plastics (Ultem 1000). MWCNTs with a reported density of 2100 kg/m^3 were obtained from Cheap Tubes (SKU #030104). The CNTs contain 98.35% C, 0.45% Cl, 0.26% Fe, and 0.96% Ni by weight per manufacturer's specifications. The transmission electron spectroscopy (TEM) analysis of the nanotubes indicated that they consist of about 20–30 concentric graphene layers (see the TEM micrographs in Fig. 1). The nanotubes exhibit an outside diameter of 30 ± 5 nm, inside diameter of 5–15 nm, and length of 10–30 μm

(hence, length/diameter, i.e., aspect ratios of about 300–1200). The concentrations of CNT in PEI used in our experiments were 1, 2, and 5% by weight [i.e., volume fractions (ϕ) of 0.006, 0.012, and 0.03, respectively]. The concentration of the CNT could not be increased beyond 5% by weight ($\phi = 0.03$) because of the difficulties associated with the adequate dispersion of the CNTs into the PEI at higher concentrations.

Attempts at Surface Functionalization

In addition to using the as-received CNT, some of the CNTs were subjected to surface functionalization. Initial functionalization attempts found excessive degradation of the CNTs when strong acids such as mixtures of nitric and sulfuric acids were used, consistent with earlier studies.[1] Acid-based modification produces functional groups such as carboxyl and hydroxide on CNTs, which typically enhances the attachment of secondary particles and some polymers on the carbon surface. Thus, a relatively weak-acid functionalization approach using citric acid[21] was used. In the functionalization procedure, citric acid monohydrate obtained from Sigma-Aldrich was used. The CNT were sonicated for 30 min within a 0.05 M citric acid solution, followed by triple rinsing with DI water, centrifuging, and drying. TEM analysis revealed that even this mild treatment gives rise to some surface and bulk damage of the CNT as shown in Figure 1. Based on the observed degradation, the CNTs were not surface functionalized prior to being incorporated into PEI.

Procedure for the Preparation of the PEI/CNT Nanocomposites

The key to optimum property enhancement of a polymer by the incorporation of CNT is proper dispersion, which can be attempted by a wide variety of methods, including melt processing via twin-screw extrusion,[22,23] high-shear intensive mixing using Banbury-type mixers,[4,24] or solution processing, typically involving the use of sonication.[25–27] The PEI has a glass transition temperature of 215 °C and is typically processed at 300–350 °C. Even at such high temperatures, Ultem 1000 has a relatively high viscosity and is a difficult material to process and does not practically allow sonication. The solution processing allows carrying out the CNT dispersion at much milder conditions using dimethyl sulfoxide (DMSO), which also has a low viscosity allowing sonication for more effective dispersion of CNTs. Previous study by Modi et al. with PEEK, another high-performance engineering plastic,[28] also showed that sonication of the low viscosity solution–based systems results in better dispersion than melt processing, which is also prone to artifacts such as degradation.

In our experiments, the CNTs were first incorporated into DMSO (99.5% purity; Sigma-Aldrich) using a Misonix XL2020 ultrasonic processor using a submerged sonic horn at a frequency of 20 kHz and in the power input range of 22.5–37.5 W. All batches used 100 g of DMSO incorporated with 0.02–0.10 g of CNT (for the 1–5% by weight PEI/CNT composites, respectively). Acoustic cavitation causes the creation, growth, and eventual collapse of bubbles within the solution with local temperatures reaching as high as 5000 K.[28] The considerable energy released by the collapse of the bubbles at such high temperatures is presumed to facilitate the exfoliation of nanotubes that arrive flocculated as a result of van der Waals forces. To ensure that the bulk temperature of the solution did not increase significantly during sonication, the temperature distributions were monitored using an Inframetrics Thermacam PM 290 thermal imaging camera. Figure 2 shows typical temperature distributions at the free surfaces of the CNT/DMSO suspension samples after 5 min of sonication under two different sets of sonication conditions (higher amplitude setting shown in the bottom image in Fig. 2). Based on the thermal imaging results, the sonication conditions were selected so that the bulk temperature could be kept at <45 °C [Fig. 2(a)]. After sonication, the nanosuspension samples were subjected to optical microscopy (Nikon, Optiphot2-POL polarizing microscope) and their linear viscoelastic material functions were characterized for assessment of the dispersion efficacy of the CNT in the DMSO.

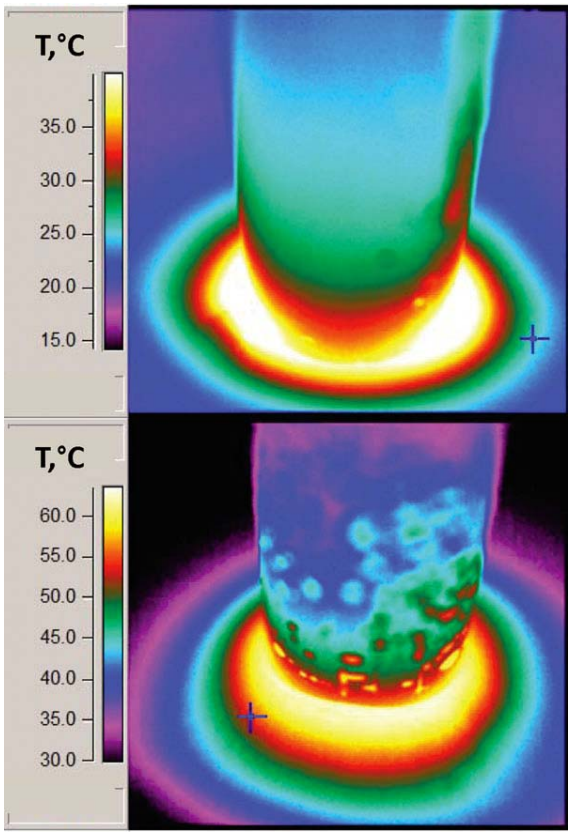

FIGURE 2 Temperature (T) distributions at the free surface of the nanosuspension during the compounding of nanotubes into DMSO (top) low power sonication, and (bottom) high power sonication.

After the CNTs were incorporated into DMSO, PEI (2.0 g) was added to the CNT/DMSO suspension under magnetic stirring. A hot plate was used to increase the mixture temperature to 165 °C. After ~35 min, all PEI pellets were dissolved. A sonic bath was used to prevent the nonhomogeneous precipitation

of the CNT with the PEI while the mixture was quenched to ambient. As the mixture cooled, a black precipitate of PEI–CNT composite formed at the bottom of the beaker. The PEI and CNT nanocomposite precipitations were filtered to remove the excess solvent and then dried in an oven for at least 1 week under vacuum at 200 °C to remove the residual solvent.

Thermogravimetric Analysis

The concentration of the remaining solvent in the CNT/PEI precipitate after drying was determined using TGA (TA Instruments Model Q50 with temperature precision and accuracy of ±0.1 °C and ±1 °C, respectively, and a balance error of ±0.01% of sample mass). At the end of the drying process, the residual solvent content was generally found to be <0.5% by weight. All PEI samples that will be referred to as "pure PEI" were processed in the same manner as controls.

An attempt was made to determine the concentration of the CNT in the specimens by using TGA in conjunction with subjecting the samples to temperature scanning up to 800 °C. Such procedures have been used in the past to determine the degree of mixedness of fillers in polymers.[29,30] However, the weight residue of the PEI remaining after exposure of PEI to temperatures as high as 800 °C was considerable, rendering it difficult to delineate the concentrations of PEI and CNT.

However, through the TGA analysis, one could recognize that the degradation temperatures of pure PEI differed from those of PEI nanocomposites. Studies have found that the CNTs can act as a thermal stabilizer that helps to decrease the flammability of polymers, decreasing the rate of oxidative degradation or delaying the onset of degradation.[31,32] The 5% CNT–PEI was found to degrade at a slower rate in the high-temperature region of 650–800 °C. After holding the sample at 800 °C for an additional 5 min, pure PEI had a mean weight residue of 1.6%, whereas 5% CNT–PEI exhibited a mean weight residue of 16.6%. Overall, these results suggest that the CNTs significantly hinder the oxidative degradation of the PEI, which is consistent with the previous literature which shows that the inclusion of the nanotubes increases the decomposition temperature.[31,33]

Sample Preparation for Rheological Characterization of Material Functions

For rheological characterization, the dried CNT/PEI samples were compression molded into disks using a Carver Press. The molding procedure for pure PEI and PEI with 1% by weight CNTs involved holding the specimen at 250 °C for 10 min with 1 metric ton of pressure, after which the samples were quenched to room temperature resulting in sample thicknesses ranging from 0.4 to 0.7 mm. The samples containing 2 and 5% CNTs were compression molded at 250 °C with 4 to 5 metric tons of pressure to achieve the same range of disk thicknesses obtained for pure PEI and PEI with 1% by weight of CNT. The rectangular torsional samples were 0.5 mm in thickness, 8–10 mm in width, and about 50 mm in length. The dimensions of each specimen were measured using a Mitutoyo micrometer (±0.001 mm) prior to being subjected to small-amplitude oscillatory shear at 21 ± 1 °C. The PEI and CNT suspensions were always maintained under agitation when dissolved in DMSO. However, once the solvent was removed, PEI was a relatively high-viscosity material in the melt state and was a lot less prone to reagglomeration due to Brownian motion and van der Waals forces, and hence, during molding and rheological characterization, reagglomeration should not be a significant issue.

Small-Amplitude Oscillatory Shear

Viscoelastic properties of PEI and PEI/CNT samples were characterized by small-amplitude oscillatory shearing using a Rheometric Scientific (currently TA Instruments) Advanced Rheometric Expansion System (ARES) Rheometer in conjunction with either 8- or 50-mm parallel-plate fixtures. The torque accuracy of the transducer of ARES is ±2 g/cm. The oven temperature could be controlled within ± 0.1 °C. In oscillatory shear, the shear strain is defined as $\gamma = \gamma^0 \sin(\omega t)$, where γ^0 is shear strain amplitude (i.e., $\gamma^0 = \theta R/h$, where θ is the maximum angular displacement, R is the disk radius, and h is the gap in between the two disks), ω is the oscillation frequency, and t is the time. The shear stress response (τ) to the imposed oscillatory deformation can be written as: $\tau = G'(\omega)\ \gamma^0 \sin(\omega t) + G''(\omega)\ \gamma^0 \cos(\omega t)$, where $G'(\omega)$ is the shear storage modulus and represents the elastic energy stored, whereas $G''(\omega)$ is the shear loss modulus and represents the energy dissipated as heat. In the region of linear viscoelasticity, the values of dynamic material properties, namely, the storage modulus, the loss modulus, and the magnitude of complex viscosity (η^*), where, $|\eta^*(\omega)| = (G'^2 + G''^2)^{0.5}$, are independent of the strain amplitude.

During small-amplitude oscillatory shearing, if changes in the dynamic properties with time occur, such changes indicate that the specimen is not stable, for example, due to crosslinking, oxidation, or hydrolysis. In small-amplitude oscillatory shear experiments, a dynamic strain sweep between strain amplitudes of 0.02 and 100% was performed at a frequency of 5 rps to determine the upper limit of the strain amplitude for the linear viscoelastic range. Time-sweep experiments were carried out on PEI and PEI/CNT nanocomposite samples to assess the stability of the specimens at 290 °C, using a frequency of 5 rps and strain amplitude of 5%. During a typical 10-min time sweep, the least-stable sample showed a storage modulus increase of about 12%, which was considered acceptable.

The dynamic properties were characterized as a function of frequency in the range of 0.1–100 rps in the linear viscoelastic range. During small-amplitude oscillatory shearing, the use of multiple frequencies allows the characterization of the linear viscoelastic response of PEI and its nanocomposites over a range of time scales, such as to provide a broad fingerprint of the viscoelastic response. In general, at relatively small characteristic times for deformation (relatively high frequencies), the elastic response is accentuated, whereas at longer characteristic times (relatively low frequencies), the viscous flow behavior is accentuated.

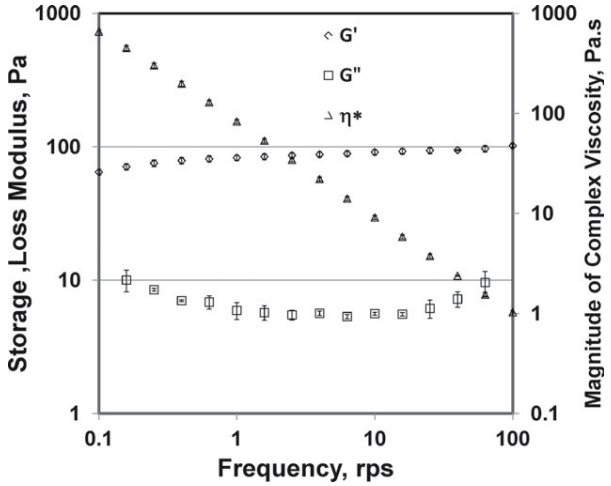

FIGURE 3 Linear viscoelastic properties storage modulus (G'), loss modulus (G''), and magnitude of complex viscosity (η^*) as a function of frequency for 1% by weight of CNT ($\phi = 0.006$) in DMSO.

Relaxation Modulus Determination

Relaxation modulus as a function of strain and time data were collected using a Rheometric Scientific ARES Rotational Rheometer in conjunction with parallel-plate fixtures with a diameter of 8 mm at 290 °C. The gap was kept constant at 0.5 mm. During the step-strain experiment, a step strain (5–200%) is applied to the polymer. The relaxation of the torque is then captured by the rheometer as the sample relaxes back to equilibrium. The step-strain experiment is inherently difficult to perform, as rapid initiation and cessation of the strain are required. In reality, ARES takes 20–30 ms to introduce the required step strain.[34] Within this time frame, complicated acceleration and deceleration of the moving fixture occur, generally rendering the relaxation data obtained for relatively small times, that is, typically <1 s, unreliable.[34]

The relaxation modulus versus time and strain data are given as follows:

$$G(t,\gamma_o) = \tau_{xy}(t)/\gamma_R \tag{1}$$

where $\tau_{xy}(t)$ is the relaxing shear stress as a function of time and γ_R is the strain at the edge of the disk, that is, $\gamma_R = \theta R/h$, where θ is the angular displacement introduced, R is the radius of the disk, and h is the gap. The nonuniformity of the shear rates in parallel-plate fixtures required a correction be made to the relaxation moduli:[35–37]

$$G(t,\gamma_R) = G_a(t,\gamma_R)\left[1+\frac{1}{4}\frac{\partial \ln G_a(t,\gamma_R)}{\partial \ln \gamma_R}\right] \tag{2}$$

where the apparent relaxation modulus $G_a(t,\gamma_R)$ is given as follows:

$$G_a(t,\gamma_R) = \frac{2T(t,\gamma_R)}{\pi R^3 \gamma_R} \tag{3}$$

where T is the torque.

Rectangular Torsional Deformation

The rectangular torsional experiments were performed using the ARES rheometer in conjunction with rectangular torsional geometry at ambient temperature. Samples with uniform thickness and width were loaded onto the fixtures, clamped, and kept under tension of ~1 N throughout the experiment at ambient temperature, that is, 21–23 °C. Strain-amplitude sweeps were performed at a frequency of 5 rps within the strain range of 0.00002–0.1%. Frequency sweeps were performed at a strain of 0.01% over the frequency range of 0.1–100 rps. For the determination of the glass transition temperature, some of the samples were subjected to small-amplitude oscillatory shearing at a constant frequency of 0.5 rps and strain amplitude of 0.1% in the temperature range 200–250 °C, also using the rectangular torsional geometry.

Paired two-tail t-tests were performed for all the experiments to determine if the differences observed in the linear viscoelastic properties of the PEI and PEI/CNT suspensions were significant or not. A 95% confidence interval was used ($\alpha = 0.05$).

RESULTS AND DISCUSSION

The frequency (ω) dependencies of the dynamic properties, that is, the storage modulus [$G'(\omega)$], the loss modulus [$G''(\omega)$], and the magnitude of complex viscosity [$\eta^*(\omega)$], of the as-received "neat" CNT incorporated into the solvent DMSO via sonication are shown in Figure 3 (1% by weight CNT in DMSO). For the entire frequency range investigated, that is, 0.1–100 rps, the storage modulus and loss modulus values are nearly parallel with $G' > G''$. Both of these traits are indicative of the gel-like behavior of the DMSO/neat CNT suspension following sonication.[38,39]

A comparison of the dynamic properties of the DMSO compounded with the as-received "neat" and surface-functionalized CNT via citric acid treatment was also made (see Fig. 4

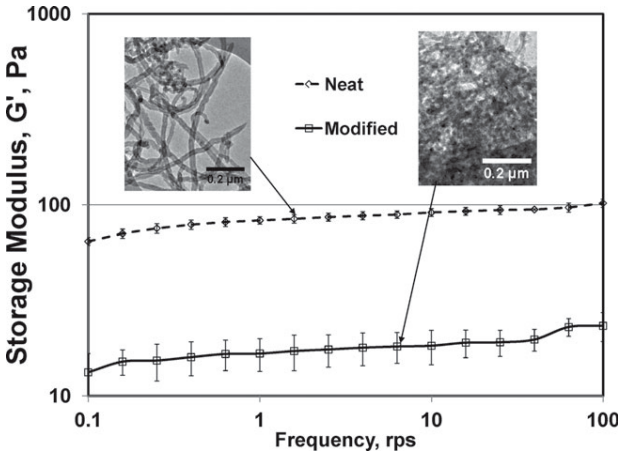

FIGURE 4 Storage modulus (G') versus frequency of 1% by weight of neat and surface-modified CNTs ($\phi = 0.006$) in DMSO. The insets show the TEM micrographs revealing a clustered state for the modified CNT.

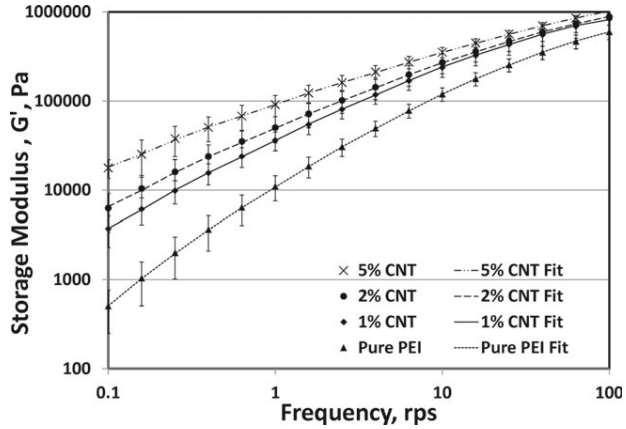

FIGURE 5 Storage modulus (G') versus frequency of suspensions of PEI with 0, 1, 2, and 5% by weight of CNT (ϕ = 0, 0.006, 0.012, 0.03) and the best fit of the generalized Maxwell model at 290 °C.

for 1% of CNT in DMSO). The functionalized CNT incorporated into DMSO also revealed a gel-like behavior ($G' > G''$ and G' and G'' independent of frequency). However, the neat CNT/DMSO suspensions exhibited significantly higher dynamic properties than the CNT/DMSO suspensions containing surface-functionalized CNT [see the storage moduli, $G'(\omega)$, values in Fig. 4]. The fivefold increase of the $G'(\omega)$ going from modified to neat CNT suggests that either there was improved dispersion of the neat CNT in DMSO (counter to expectations) or because the aspect ratios of the modified CNT were reduced during the citric acid-functionalization process. TEM analysis indicated that the aspect ratios of functionalized CNTs were indeed about an order of magnitude smaller than the neat CNT and that the neat CNTs were better exfoliated on sonication (see insets in Fig. 4). Considering that the aspect ratios could be better preserved and the nanotubes could be better dispersed for the case of the neat CNT, the rest of our investigation, reported in Figures 5–15, used only neat CNT.

Dynamic Properties of CNT in PEI in Melt State

Dynamic properties, that is, the storage modulus [$G'(\omega)$], the loss modulus [$G''(\omega)$], and the magnitude of complex viscosity [$\eta^*(\omega)$], of the PEI and PEI/CNT nanosuspensions with 0, 1, 2, and 5% by weight of CNT (volume fraction ϕ in the range of 0–0.03) were collected. Storage modulus versus frequency behavior of the PEI and its suspensions are shown in Figure 5 at 290 °C. The storage modulus increases with increasing CNT concentration, with the increase most prominent at a CNT concentration of 5%. Pure PEI has a modulus of 505 ± 39 Pa at ω = 0.1 rps, and the addition of 1% CNT raises this value to 3712 ± 1425 Pa. Doubling the CNT content to 2% by weight yields a storage modulus of 6300 ± 2890 Pa, and raising it to 5% gives a modulus of 17,772 ± 4221 Pa for 0.1 rps. Paired two-tailed *t*-tests on the pure PEI/5% CNT and 2% CNT/5% CNT and 1% CNT/2% CNT show that the increase in storage modulus due to the addition of CNT is significant at a *p*-value of 0.05. Such observed increases of the elasticity and the viscosity of CNT/PEI suspensions were also reported for other thermoplastic polymer/CNT composites, such as the 2 orders of magnitude increase in storage modulus of poly(carbonate) composites observed for 5% by weight CNT,[9] and the 3–4 orders of magnitude increase for poly(ethylene terephthalate) with 4.8% CNT.[40] An order of magnitude difference in storage modulus exists between PEI with 1% CNT and pure PEI, suggesting that rheological percolation has been achieved with the PEI with 1% CNT (CNT volume fraction, ϕ = 0.006). This is consistent with the consideration that the transition from dilute to the concentrated isotropic concentration regime (at which the CNTs begin to have difficulty packing isotropically) occurs at $\varphi \approx \frac{\pi d}{4L}$, that is, $O(10^{-3})$.[41] Increases similar to those observed for the storage modulus values were also observed for the loss modulus values of PEI versus PEI/CNT suspensions (Fig. 6).

The dynamic properties, that is, the storage modulus and loss modulus values were analyzed in conjunction with a linear viscoelastic model, the generalized Maxwell constitutive equation, to determine the relaxation time versus the relaxation strength spectra of PEI and PEI/CNT nanosuspensions. According to the generalized Maxwell model, the storage and loss moduli are given as follows:[42]

$$G'(\omega) = \sum_i \frac{G_{oi}\lambda_i^2\omega^2}{1+\lambda_i^2\omega^2} \tag{4}$$

$$G''(\omega) = \sum_i \frac{G_{oi}\lambda_i\omega}{1+\lambda_i^2\omega^2} \tag{5}$$

Relaxation times and relaxation strengths were determined by minimizing the objective function:[20]

$$F = \sum_{i=1}^{N} \left\{ \left[\left(G'_{i,exp} - G'_{i,fit} \right) / G'_{i,exp} \right]^2 + \left[\left(G''_{i,exp} - G''_{i,fit} \right) / G''_{i,exp} \right]^2 \right\} \tag{6}$$

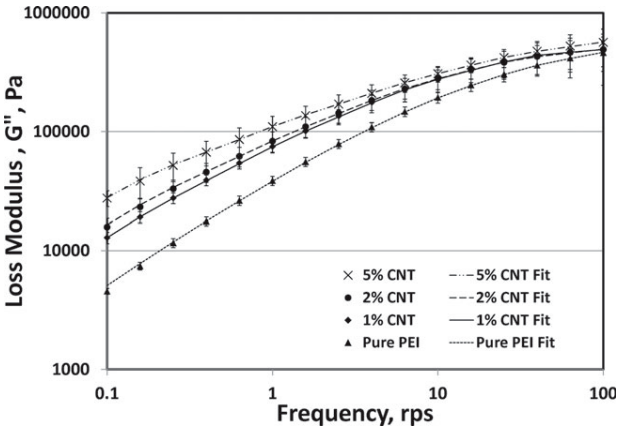

FIGURE 6 Loss modulus (G'') versus frequency of suspensions of PEI with 0, 1, 2, and 5% by weight of CNT (ϕ = 0, 0.006, 0.012, 0.03) and the best fit of the generalized Maxwell model at 290 °C.

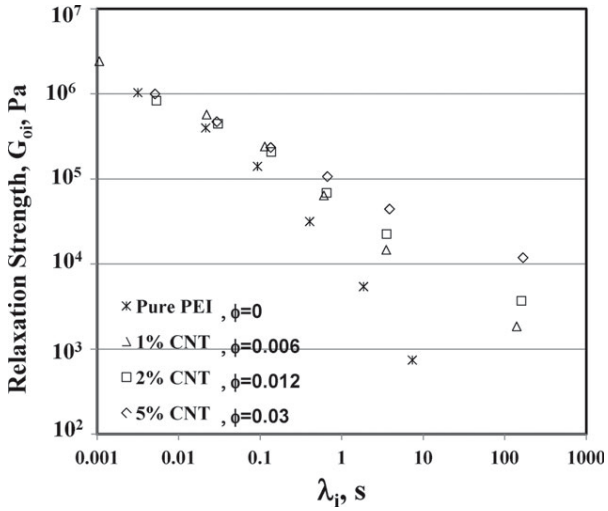

FIGURE 7 Relaxation strength (G_{oi}) versus the relaxation time (λ_i) spectra of PEI and suspensions of PEI with 0–5% by weight of CNT (ϕ = 0, 0.006, 0.012, 0.03) at 290 °C.

where N is the number of data points, $G'_{i,exp}$ and $G''_{i,exp}$ are the experimental data obtained from the frequency sweeps, and $G'_{i,fit}$ and $G''_{i,fit}$ are determined on the basis of a generalized Maxwell model.[20]

The best-fit values of the relaxation time, λ_i, versus relaxation strength, G_{oi}, are shown in Figure 7. The relaxation time and strength values increase with increasing concentration of the CNTs. The comparisons of the best fits of the generalized Maxwell model and the experimental data for the storage modulus [$G'(\omega)$] and the loss modulus [$G''(\omega)$] are shown in Figures 5 and 6, respectively, and the fit is acceptable. The relaxation spectra obtained from the dynamic properties with the generalized Maxwell model provides the basic wherewithal, along with the fitting of the damping function obtained from the step-strain experiments, for the utilization

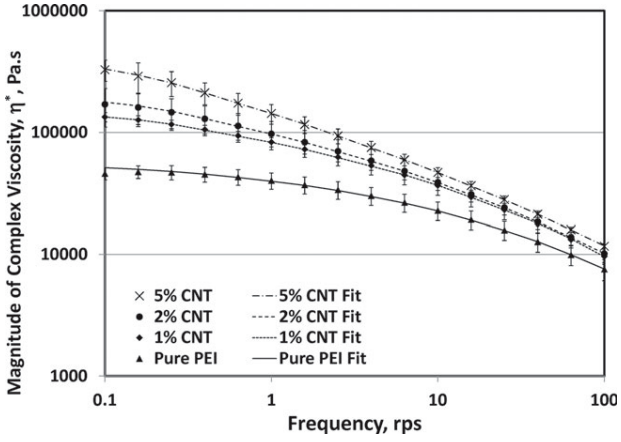

FIGURE 8 Magnitude of complex viscosity of PEI and PEI suspensions with 1, 2, and 5% by weight of CNT (ϕ = 0, 0.006, 0.012, 0.03) versus frequency and comparisons with the predictions of the generalized Maxwell model at 290 °C.

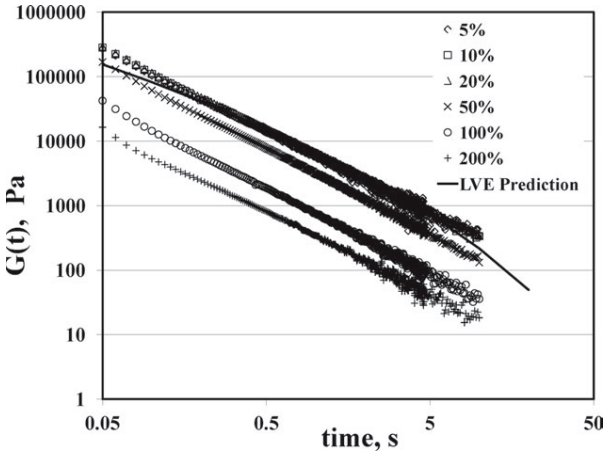

FIGURE 9 Stress relaxation on imposition of step strain for pure PEI and predictions of the generalized Maxwell model at 290 °C.

of a nonlinear viscoelastic constitutive equation as will be later discussed.

The predicted zero-shear viscosity values of PEI and PEI/CNT suspensions, that is, $\eta_0 = \sum_i G_{oi}\lambda_{oi}$, were determined as 5.3×10^4, 2.7×10^5, 7.4×10^5, and 2.3×10^6 for 0, 1, 2, and 5% by weight of CNT, respectively. The 1–2 orders of magnitude increase in the shear viscosity of the nanocomposite with modest increases in the concentration of CNT, that is, 1–5% by weight, is indicative of the challenging nature of the preparation of polymeric nanocomposites. The comparison of the predicted zero-shear viscosity values with the magnitude of complex viscosity values (Fig. 8) as the frequency approaches zero for 0–2% CNT indicates that the Cox-Mertz rule is approached, that is, the shear viscosity and the magnitude of complex viscosity approach each other as the shear rate and the frequency both approach zero. However, the Cox-Mertz rule does not hold for PEI with 5% CNT, that is, the predicted zero-shear viscosity is observed to be significantly higher than the magnitude of complex viscosity values at low frequencies.

Relaxation Modulus Behavior at 290 °C as Characterized with Step-Strain Experiments

Step-strain experiments were performed at varying strains, $\gamma = \theta R/H$, where θ is the angular displacement, R is the radius, and H is the gap of the parallel plates used for the step-strain experiments. The strains were varied from 5, 10, 20, 50, 100, and 200% at 290 °C, and the relaxation modulus versus time and strain behavior data were collected (Figs. 9 and 10). The step-strain experiments were performed on the pure, 1% (Figs. 9 and 10), 2%, and 5% CNT–PEI samples, all of which became nonlinear at about 50% strain, that is, the relaxation modulus curve for 50% ceased to overlap with those of lower strains. The time-dependent relaxation modulus as a function of time [$G(t)$] behavior of PEI and its suspensions could be predicted in the linear viscoelastic range on the basis of the relaxation spectra (G_{oi} vs. λ_i, reported in

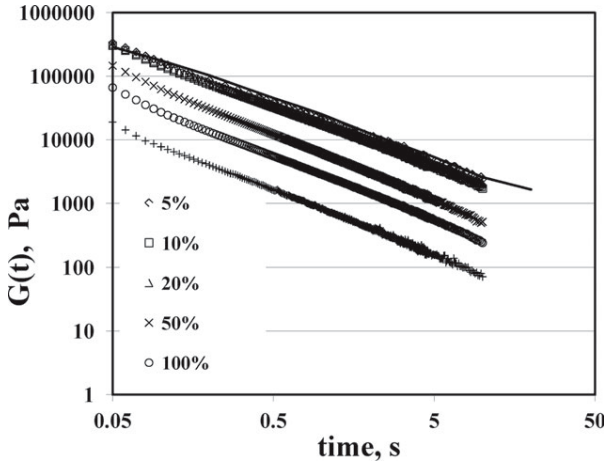

FIGURE 10 Stress relaxation on imposition of step strain for PEI with 1% by weight CNT ($\phi = 0.006$) and predictions of the linear viscoelasticity, that is, generalized Maxwell model at 290 °C.

Fig. 7) obtained from the best Maxwellian fit of the dynamic properties:[42]

$$G(t) = \sum_i G_{oi} \exp(-t/\lambda_i) \quad (7)$$

Figures 9 and 10 show the comparisons of the relaxation moduli obtained from the generalized Maxwell model (eq. 7) versus the experimental data collected with the step-strain experiments in the linear range for pure PEI and 1% by weight CNT ($\phi = 0.006$). The agreement is excellent for the PEI and PEI with 1 and 2% by weight of CNT ($\phi = 0.006$ and 0.012). On the other hand, the predicted relaxation modulus values are considerably higher than the experimental ones for PEI with 5% CNT ($\phi = 0.03$). This large deviation between the prediction of the generalized Maxwell model versus experimental data for $\phi = 0.03$ is consistent with the comparison of the zero-shear viscosity values versus the magnitude of complex viscosity as the frequency approaches zero (as discussed earlier), in which the predicted zero-shear viscosity was determined to be significantly higher than the magnitude of complex viscosity as the frequency approaches zero for the 5% CNT samples. These differences observed for the 5% CNT–PEI sample likely stem from the formation of a yield stress, as noted earlier, which should also lead to strong wall slip of the 5% suspension with the highest concentration of CNT, an effect which is well documented for various polymers and polymeric suspension systems.[34,43,44]

The damping function $h(\gamma) = G(t,\gamma)/G(t)$ versus γ behavior of the PEI melt and PEI nanosuspensions are shown in Figure 11. The damping function $h(\gamma)$ data were fitted with a single exponential $[h(\gamma) = \exp(-n\gamma)]$ with the n values determined to be in the range of 1.5–2.0. The nanosuspension samples typically relax at a slower rate with increasing concentration of CNT, which can be attributed to the decreased mobility, that is, confinement effect, of the macromolecules in the presence of CNTs on one hand and the formation of a CNT network that spans the volume of the sample on the other as noted earlier for the highest CNT concentration of 5% by weight ($\phi = 0.03$). With increasing CNT concentration, the CNT mesh becomes more interconnected, providing additional affine junctions[45] that further increase the relaxation times of the suspensions and the relaxation modulus in the linear viscoelastic range observed on the Maxwellian fit. The formation of the network will be influenced by the state of the dispersion and exfoliation of the nanoparticles.[46] The decrease of the polymer chain mobility in the presence of CNTs has also been observed to influence the mechanical properties of polymer nanocomposites at temperatures below the glass transition of the nanocomposite.[47,48]

The predictions of the shear viscosity $[\eta(\dot{\gamma})]$ and the first normal stress difference $[N_1(\dot{\gamma})]$ as a function of the shear rate $(\dot{\gamma})$ at 290 °C could be made on the basis of using a time-strain separable (with a kernel consisting of a memory function depending only on time and a damping function depending only on strain) integral-type viscoelastic constitutive equation, that is, the Wagner postulate of K-BKZ constitutive equation.[49,50] The material functions of the K-BKZ equation were given by Kalyon et al. for an exponential damping function:[20]

$$\eta(\dot{\gamma}) = \sum \frac{G_{o,i}\lambda_i}{(1+n\dot{\gamma}\lambda_i)^2} \text{ and } N_1(\dot{\gamma}) = \dot{\gamma}^2 \sum \frac{2G_{o,i}\lambda_i^2}{(1+n\dot{\gamma}\lambda_i)^3} \quad (8)$$

The K-BKZ equation can be used for the analysis of the thermomechanical histories that are developed during the processing of PEI nanocomposites similar to what could be demonstrated for pure PEI.[51–54]

The material functions of $\eta(\dot{\gamma})$ and $N_1(\dot{\gamma})$ predicted from the K-BKZ constitutive equation are shown in Figures 12 and 13. The shear viscosity and the elasticity of the nanosuspensions are predicted to increase significantly, especially at the low shear rate range on the incorporation of the CNT into the PEI melt, rendering it more difficult to process and shape

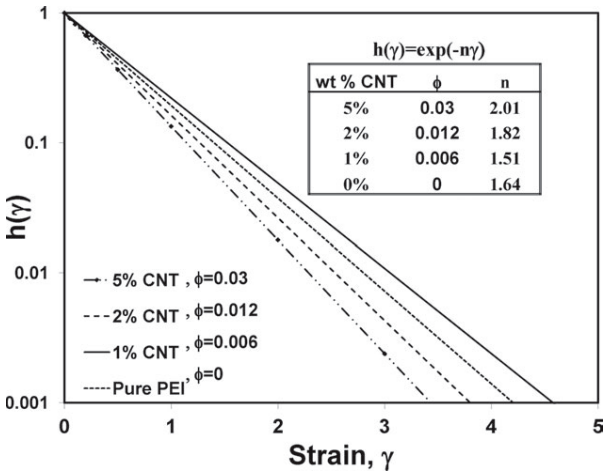

FIGURE 11 Damping function values of PEI and its CNT nanosuspensions at 290 °C.

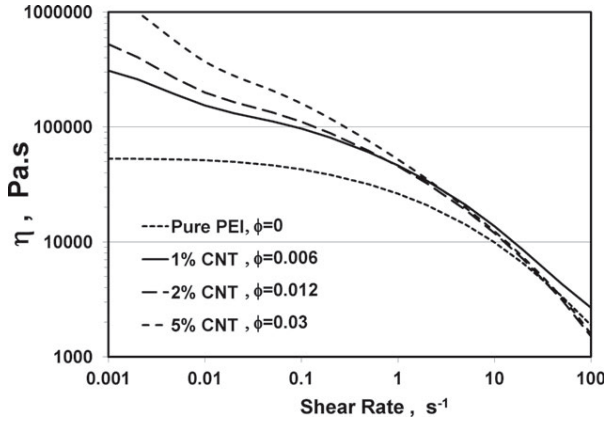

FIGURE 12 Predicted shear viscosity material function of PEI and its CNT nanosuspensions at 290 °C.

the PEI nanosuspensions as the concentration of the CNT increases. Predictions of the integral-type viscoelastic constitutive equation for the CNT/PEI suspension with 5% by weight CNT ($\phi = 0.03$) suggests that a relatively high yield stress is developed at this high concentration.

The dynamic properties of the pure PEI and PEI nanocomposites were further characterized at 25 °C using the rectangular torsional fixtures. As shown in Figure 14, the PEI/CNT nanocomposites exhibit an increase in storage modulus with increasing CNT concentration. However, the increase in the modulus obtained in the glassy state (below the glass transition temperature) is not as marked as the increase in storage modulus that is observed in the melt state as discussed earlier. The 5% CNT samples show the greatest increase, with the modulus increasing from $1.5 \times 10^9 \pm 2.4 \times 10^7$ Pa to about $2.3 \times 10^9 \pm 2.1 \times 10^7$ Pa (about a 54% increase). Two-tailed tests indicated that the results were statistically significant for PEI versus PEI with 2% CNT and PEI with 2% CNT versus PEI with 5% CNT at a p-value of 0.05. A 95% increase in the loss modulus (G'') was observed, as well as a 26% increase in tan δ for the PEI with 5% CNT.

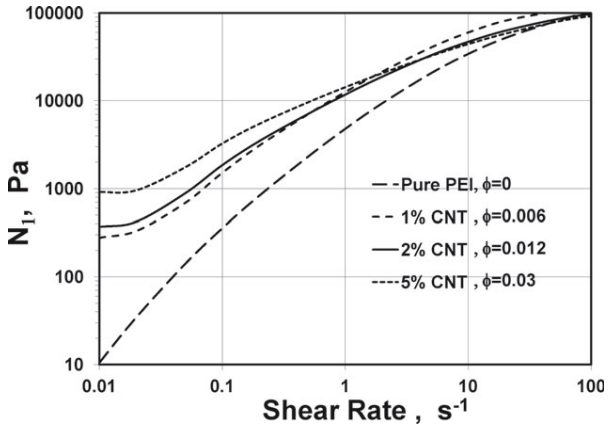

FIGURE 13 Predicted first normal stress difference material function of PEI and its CNT nanosuspensions at 290 °C

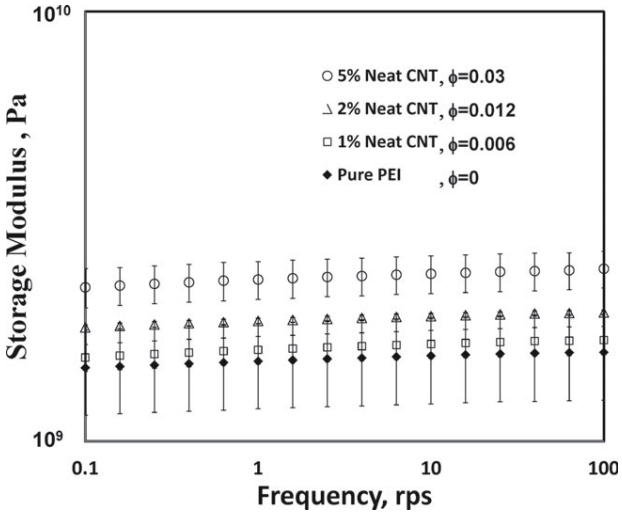

FIGURE 14 Storage modulus versus frequency of PEI nanosuspensions at different CNT concentrations at ambient temperature.

The dynamic properties of the PEI and PEI nanocomposite samples were also characterized as a function of temperature by keeping the frequency and the strain amplitude constant in the temperature range of 200–220 °C (Fig. 15). At 200 °C, PEI has a storage modulus of 1.14×10^9 Pa, whereas the PEI with 5% CNT has a storage modulus of 2.06×10^9 Pa. The significant decrease in modulus observed (normalized in terms of the storage modulus at 200 °C) in the 200–220 °C temperature range is associated with the transition of the PEI and PEI nanocomposites from the glassy to the rubbery states. In these experiments, multiple rates of temperature ramping were used (0.5–5 °C/min), and the results reported here pertain to the ramping-rate-independent sets of data. Both the PEI and PEI with 5% CNT exhibited relatively broad decreases in storage modulus. The glass transition temperature can be determined from the

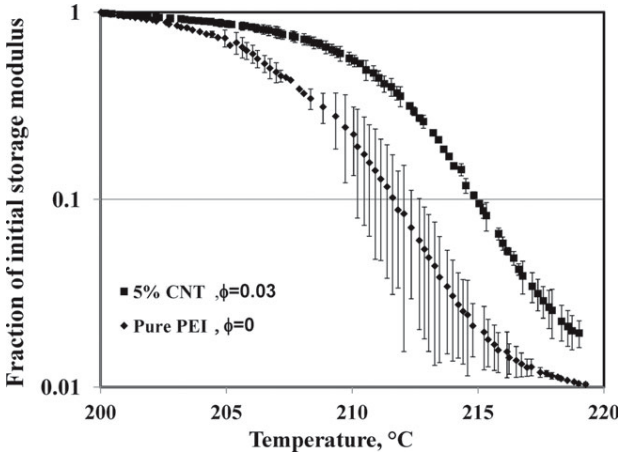

FIGURE 15 Ratio of storage modulus at various temperatures over the storage modulus at 200 °C versus temperature for PEI and PEI with 5% of CNT ($\phi = 0.03$).

maximum of the tan $\delta = G''/G'$ as a function of temperature. In addition, the glass transition temperature values for pure PEI and 5% CNT–PEI were found to differ significantly using a two-tailed test with a p-value of 0.05 (a 4 °C increase from 214 to 218 °C on the incorporation of the CNT). Engineering plastics like PEI exhibit complex microstructures on processing,[51–54] and the incorporation of CNT will further complicate the thermomechanical history to be experienced by the PEI nanosuspensions and the microstructural distributions resulting from the processing operation.

CONCLUSIONS

The changes in the temperature-dependent viscoelastic behavior of an amorphous engineering plastic like PEI on the solution-based incorporation of MWCNTs were investigated. The viscoelastic material functions included the dynamic properties obtained via small-amplitude oscillatory shear over a broad range of temperatures and relaxation moduli of the PEI melts using step strain. The weight fractions of CNT were 1, 2, and 5% (volume fractions, $\phi =$ 0.006, 0.012, and 0.03). During attempts for surface functionalization of the CNT, even a relatively mild treatment involving 0.05 M citric acid gave rise to some bulk and surface damage of the CNT (leading to surface treatment being avoided during sample preparation). The neat CNT could be dispersed into DMSO solvent using the dynamic properties of the solvent/CNT mixtures as a litmus test for the adequacy of the dispersion method. A thermal imaging camera was used to avoid application of sonication conditions under which temperature hotspots developed during sonication.

The incorporation of the CNTs increased the elasticity and the shear viscosity significantly, for example, more than 35-fold increase in storage modulus and 800% increase in the magnitude of complex viscosity were observed for PEI with 5% CNT ($\phi = 0.03$) versus pure PEI at 290 °C, indicative of the formation of a network of CNT that span the volume of the nanosuspensions at this CNT concentration. The incorporation of the CNTs decreased the mobility of the PEI leading to increases in the relaxation times and the relaxation strengths and relaxation moduli with increasing CNT concentration in the melt. At ambient temperature, the increases in moduli of the rectangular torsional samples were more modest, for example, the storage modulus showed a 54% increase for PEI with 5% CNT samples versus pure PEI, indicative of the complications associated with solidification and structure formation on molding of the specimens. The glass transition temperature increased by 4 °C with the incorporation of 5% by weight CNT.

A generalized Maxwell model was found to be adequate to describe the linear viscoelastic behavior of PEI and PEI with 1 and 2% by weight CNT but failed at 5% (ϕ=0.03), presumably due to the formation of a strong CNT network and possible onset of wall slip. A nonlinear viscoelastic constitutive equation, K-BKZ, was used (on fitting its parameters, i.e., damping function from step strain and memory function from relaxation spectra fitted from the dynamic properties) to predict the shear viscosity and elasticity (first normal stress difference) behavior at temperatures and shear rates that are typical of processing of the nanocomposites of PEI/CNT and reflected the expected increase in the difficulty of the processability of the nanocomposites with increasing CNT concentrations. Finally, the CNTs significantly hindered the oxidative degradation of the PEI, that is, the inclusion of the nanotubes increased the decomposition temperature of PEI.

ACKNOWLEDGMENTS

This study was funded by the US Army ARDEC at Picatinny Arsenal, NJ. The authors thank Kenneth Kim of ARDEC, Gaurav Mago of Lubrizol, Inc., and Semra Senturk and Asli Ergun of Stevens Institute of Technology for their help and input.

REFERENCES AND NOTES

1 Kumar, S.; Rath, T.; Mahaling, R. N.; Reddy, C. S.; Das, C. K.; Pandey, K. N.; Srivastava, R. B.; Yadaw, S. B. *Mater. Sci. Eng. B* **2007,** *141*, 61–70.

2 Ajayan, P. M.; Tour, J. M. *Nature* **2007,** *447*, 1066–1068.

3 Kearns, J.; Shambaugh, R. *J. Appl. Polym. Sci.* **2002,** *86*, 2079–2084.

4 Lozano, K.; Barera, E. V. *J. Appl. Polym. Sci.* **2001,** *79*, 125–133.

5 Seo, M. K.; Park, S. J. *Chem. Phys. Lett.* **2004,** *395*, 44–48.

6 Cooper, C. A.; Ravich, D.; Lips, D.; Mayer, D.; Wagner, H. *Compos. Sci. Technol.* **2002,** *62*, 1105–1112.

7 Jin, Z.; Pramoda, K.; Xu, G.; Goh, S. H. *Chem. Phys. Lett.* **2001,** *337*, 43–47.

8 Ma, H.; Zeng, J.; Kumar, S.; Schiraldi, D. *Compos. Sci. Technol.* **2003,** *63*, 1617–1628.

9 Potschke, P.; Fornes, T. D.; Paul, D. R. *Polymer* **2002,** *43*, 3247–3255.

10 Sennett, M.; Welsh, E.; Bright, J. B.; Li, W.; Wen, J. G.; Ren, Z. F. *Appl. Phys. A* **2003,** *76*, 111–113.

11 Xiao, K. Q.; Zhang, L. C.; Zarudi, I. *Compos. Sci. Technol.* **2007,** *67*, 177–182.

12 Cai, H.; Yan, F.; Xue, Q. *Mater. Sci. Eng. A* **2004,** *364*, 94–100.

13 Sandler, J.; Windle, A. H.; Werner, P.; Altstadt, V.; Es, M. V.; Shaffer, M. S. P. *J. Mater. Sci.* **2003,** *38*, 2135–2141.

14 Mago, G.; Fisher, F. T.; Kalyon, D. M. *J. Nanosci. Nanotechnol.* **2009,** *9*, 3330–3340.

15 Mago, G.; Fisher, F. T.; Kalyon, D. M. *J. Nanomater.* **2008,** *1–8*, 759825.

16 Kumar, S.; Li, B.; Caceres, S.; Maguire, R. G.; Zhong, W. H. *Nanotechnology* **2009,** *20*, 1–8.

17 Liu, T.; Tong, Y.; Zhang, W. D. *Compos. Sci. Technol.* **2007,** *67*, 406–412.

18 Hough, L. A.; Islam, M. F.; Janmey, P. A.; Yodh, A. G. *Phys. Rev. Lett.* **2004,** *93*, 168102–1168102–4.

19 Ma, W. K.; Chinesta, F.; Ammar, A.; Mackley, M. R. *J. Rheol.* **2008,** *52*, 1311–1330.

20 Kalyon, D. M.; Yu, D. W.; Yu, J. S. *J. Rheol.* **1988,** *32*, 789–811.

21 Poh, C. K.; Lim, S. H.; Pan, H.; Lin, J.; Lee, J. Y. *J. Power Sources* **2008,** *176*, 70–75.

22 Carneiro, O. S.; Covas, J. A.; Bernardo, C. A.; Caldiera, G.; Van Hattum, F. W. J.; Ting, J. M.; Alig, R. L.; Lake, M. L. *Compos. Sci. Technol.* **1998,** *51*, 401.

23 Caldiera, G.; Maia, J. M.; Carneiro, O. S.; Covas, J. A.; Bernardo, C. A. *Polym. Compos.* **2004,** *19*, 147–151.

24 Mago, G.; Fisher, F. T.; Kalyon, D. M. *Macromolecules* **2008,** *41*, 8103–8113.

25 Mago, G.; Kalyon, D. M.; Fisher, F. T. *J. Appl. Polym. Sci.* **2009,** *114*, 1312–1319.

26 Moniruzzaman, M.; Winey, K. I. *Macromolecules* **2006,** *39*, 5194–5205.

27 Velasco-Santos, C.; Martinez-Hernandez, A. L.; Fisher, F. T.; Ruoff, R.; Castano, V. M. *J. Phys. D: Appl. Phys.* **2003,** *36*, 1423–1428.

28 Modi, S. H.; Dikovics, K. B.; Gevgilili, H.; Mago, G.; Bartolucci, S.; Fisher, F. T.; Kalyon, D. M. *Polymer* **2010,** *51*, 5236–5244.

29 Erol, M.; Kalyon, D. M. *Int. Polym. Process.* **2005,** *3*, 228–237.

30 Kalyon, D. M.; Dalwadi, D.; Erol, M.; Birinci, E.; Tsenoglu, C. *Rheol. Acta* **2006,** *45*, 641–658.

31 Kashiwagi, T.; Du, F.; Douglas, J. F.; Winey, K. I.; Harris, R. H., Jr.; Shields, J. R. *Nat. Mater.* **2005,** *4*, 928–933.

32 Schartel, B.; Pötschke, P.; Knoll, U.; Abdel-Goad, M. *Eur. Polym. J.* **2005,** *41*, 1061–1070.

33 Du, F.; Fischer, J. E.; Winey, K. I. *J. Polym. Sci. Part B: Polym. Phys.* **2003,** *41*, 3333–3338.

34 Gevgilili, H.; Kalyon, D. M. *J. Rheol.* **2001,** *45*, 467–475.

35 Nadai, A. Plasticity: A Mechanics of the Plastic State of Matter; McGraw Hill: New York, **1931;** pp 126–128.

36 Penn, R.; Kearsley, E. *Trans. Soc. Rheol.* **1976,** *20*, 227–238.

37 Soskey, P.; Winter, H. *J. Rheol.* **1984,** *26*, 625–645.

38 Chambon, F.; Winter, H. H. *J. Rheol.* **1987,** *31*, 683–697.

39 DeRosa, M. E.; Winter, H. H. *Rheol. Acta* **1994,** *33*, 220–237.

40 Hu, G.; Zhao, C.; Zhang, S.; Yang, M.; Wang, Z. *Polymer* **2005,** *47*, 480–488.

41 Larson, R. Structure and Rheology of Complex Fluids; Oxford University Press: New York, **1999.**

42 Bird, R. B.; Armstrong, R. C.; Hassager, O. Dynamics of Polymeric Liquids; Wiley: New York, **1987; Vol.** *1*.

43 Yilmazer, U.; Kalyon, D. M. *J. Rheol.* **1989,** *33*, 1197–1212.

44 Aral, B. K.; Kalyon, D. M. *J. Rheol.* **1994,** *38*, 957–972.

45 Lodge, A. S.Elastic Liquids; Academic Press: New York, **1964.**

46 Batthacharya, S. N.; Kamal, M.; Gupta, R. Polymeric Nanocomposites: Theory and Practice; Carl Hanser Verlag: Munich, **2007.**

47 Eitan, A.; Fisher, F. T.; Andrews, R.; Brinson, L. C.; Schadler, L. S. *Compos. Sci. Technol.* **2006,** *66*, 1159–1170.

48 Fisher, F. T.; Eitan, A.; Andrews, R.; Brinson, L. C.; Schadler, L. S. *Adv. Compos. Lett.* **2004,** *13*, 105–111.

49 Bernstein, B.; Kearsley, E.; Zapas, L. *Trans. Soc. Rheol.* **1963,** *7*, 391–410.

50 Wagner, M. H. *Rheol. Acta* **1976,** *15*, 136–142.

51 Yu, J. S.; Wagner, A. H.; Kalyon, D. M. *J. Appl. Polym. Sci.* **1992,** *44*, 477–489.

52 Yu, J.; Kalyon, D. M. *Polym. Eng. Sci.* **1991,** *31*, 153–160.

53 Wagner, H.; Kalyon, D. M. *Polym. Eng. Sci.* **1991,** *21*, 1393–1399.

54 Wagner, A.; Yu, J.; Kalyon, D. M. *Adv. Polym. Tech.* **1989,** *9*, 17–32.

55 Gedanken, A. *Ultrason. Sonochem.* **2004,** *11*, 47–55.